

Unsupervised Graph-based Learning Method for Sub-band Allocation in 6G Subnetworks

Daniel Abode^{1,2}, Ramoni Adeogun¹, Lou Salaün³, Renato Abreu², Thomas Jacobsen², Gilberto Berardinelli¹

¹*Department of Electronic Systems, Aalborg University, Denmark.*

²*Nokia, Aalborg, Denmark.*

³*Nokia Bell Labs, Massy, France*

Email:^{1,2}{danieloa, ra, gb}@es.aau.dk, ²renato.abreu@nokia.com, ²thomas.jacobsen@nokia.com,

³lou.salaun@nokia-bell-labs.com

Abstract—In this paper, we present an unsupervised approach for frequency sub-band allocation in wireless networks using graph-based learning. We consider a dense deployment of sub-networks in the factory environment with a limited number of sub-bands which must be optimally allocated to coordinate inter-subnetwork interference. We model the subnetwork deployment as a conflict graph and propose an unsupervised learning approach inspired by the graph colouring heuristic and the Potts model to optimize the sub-band allocation using graph neural networks. The numerical evaluation shows that the proposed method achieves close performance to the centralized greedy colouring sub-band allocation heuristic with lower computational time complexity. In addition, it incurs reduced signalling overhead compared to iterative optimization heuristics that require all the mutual interfering channel information. We further demonstrate that the method is robust to different network settings.

Index Terms—Sub-band allocation, interference coordination, graph neural networks, subnetworks.

I. INTRODUCTION

The densification of wireless networks is necessary to support the growing connectivity demand, a trend that will continue towards 6G [1]. The authors in [2] envisioned 6G to be a 'network of networks', where autonomous short-range low-power subnetworks inside entities such as vehicles, robots, industrial modules etc. can offload local communication within the entities from the central network. In addition, other network architectures, such as unmanned aerial vehicle communication, and private cells are also being developed. However, the increasing density, mobility, and uncoordinated deployment of cells would increase the strain on available radio resources, demanding the need for dynamic and efficient approaches to managing them. These radio resources include power, space, time and frequency. The latter is the focus of this paper.

The typical approach to managing the frequency resources involves dividing the available bandwidth into sub-bands to be reused at different cells in the network. Frequency reuse

is crucial to balance the tradeoff between maximizing the cellular network's ability to accommodate more users and mitigating interference [3]. However, the number of sub-bands is usually limited compared to the number of cells. Hence, optimally allocating the sub-bands results in a combinatorial optimization problem which is known to be NP-hard [3]. As a consequence, various sub-optimal heuristics and data-driven solutions have been developed.

The sub-band allocation can be formulated as a graph colouring problem as in [4]–[6], where APs or cells are represented as nodes in a graph and the edges model mutual interference. The graph colouring problem defines the assignment of colours (sub-bands) to nodes (AP or cell) such that no nodes connected by an edge (i.e., adjacent nodes) are assigned the same colour [7]. The approach of formulating sub-band allocation as a graph colouring problem is advantageous because wireless networks can be naturally represented as graphs. Additionally, graph colouring has been extensively studied, resulting in a variety of proposed solutions. A common approach is to use a sub-optimal greedy colouring algorithm since exact solutions are typically exponential in complexity [8]. This approach has been considered for sub-band allocation in ultra-dense networks, femtocells and subnetworks in [4]–[6]. It has also been widely adopted for sub-band allocation in Wireless Local Area Network (WLAN) [9]. Compared to other iterative heuristics like simulated annealing [10] and Sequential Iterative Subband Allocation (SISA) [11], greedy colouring algorithms are less computationally complex [4]. Nevertheless, there is growing interest in solving the sub-band allocation problem using data-driven methods, mainly motivated by the reduction in computational complexity offered by such approaches [9], [12]–[15]. Typically, most data-driven approaches model sub-band allocation as a mixed integer optimization problem solved by supervised learning, unsupervised learning or reinforcement learning with loss function and input features characterized by the channel gain information.

This paper presents a novel unsupervised approach to sub-band allocation using graph-based learning. Our approach is inspired by the graph colouring heuristic and utilizes a loss function based on the Potts model which learns to penalize adjacent nodes allocating the same sub-band, hence the loss function does not depend on the channel gain information

The work by Daniel Abode was supported by the Horizon 2020 research and innovation programme under the Marie Skłodowska-Curie grant agreement No. 956670. The work by Gilberto Berardinelli, Renato Abreu, Thomas Jacobsen, and Ramoni Adeogun was supported by the HORIZON-JU-SNS-2022-STREAM-B-01-03 6G-SHINE project (grant agreement No. 101095738). Ramoni Adeogun's work was also partly supported by HORIZON-JU-SNS-2022-STREAM-B-01-02 project - CENTRIC (grant agreement No. 101096379)

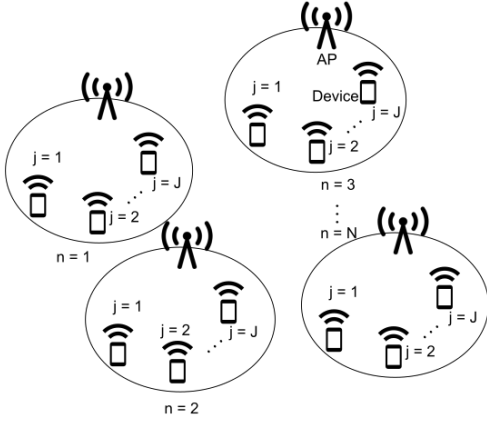


Fig. 1. Deployment of N subnetworks with J devices

for training. We employ a Graph Neural Network (GNN) as the graph-based learning model. The GNN is permutation-equivariant, scalable to changes in the size of the wireless network, and robust to different channel measurements. In addition, it can be executed in a centralized or decentralized manner. In this regard, our major contributions are as follows;

- We represent the subnetworks deployment as a conflict graph considering two graph construction rules based on information on mutual interference and signal-to-interference ratio.
- We model the sub-band allocation as a node classification task and propose an unsupervised graph-based learning approach inspired by the Potts model.
- We conduct extensive simulations to evaluate the performance and complexity of the approach compared to heuristic benchmarks. Furthermore, we evaluate the generalizability of the approach to different numbers of subnetworks, deployment density and channel models.

The rest of the paper is structured as follows. The next section presents the subnetwork system model and the problem formulation for sub-band allocation. In Section III, we describe the proposed GNN algorithm followed by the performance evaluation and the simulation assumption in Section IV. Finally, we give some concluding remarks and future direction in Section V.

II. SYSTEM MODEL AND PROBLEM FORMULATION

A. Subnetworks System Model

We consider a network of $\mathcal{N} = \{1, 2, 3, \dots, N\}$ subnetworks which are densely and randomly deployed in an area as shown in figure 1 [6]. Each subnetwork consists of an access point (AP) that coordinates the communication of its $\mathcal{J} = \{1, 2, \dots, J\}$ connected devices. The subnetwork and devices are indexed with $n \in \mathcal{N}$ and $j \in \mathcal{J}$ respectively. We assume that the subnetworks operate over a synchronized time-frequency resource grid with the available bandwidth divided into K orthogonal sub-bands, where $K \ll N$. Hence, the K sub-bands are expected to be reused by multiple subnetworks,

generating mutual interference. The sub-bands allocated to a subnetwork are further partitioned into orthogonal time-frequency slots so that each device in a subnetwork is allocated a dedicated time-frequency slot to avoid intra-subnetwork interference. We assume that each subnetwork can be allocated only one sub-band $k \in \{1, 2, \dots, K\}$, which is identified by a one-hot encoded vector $\theta_n \in \mathbb{B}^K$. Hence, for the network of N subnetworks, we can define a sub-band selection matrix $\Theta \in \mathbb{B}^{K \times N}$, such that $\theta_n = \Theta[:, n]$. The SINR of the uplink transmission between the j th device and the AP in subnetwork n occupying a channel slot in sub-band θ_n , with a channel gain, $\gamma_{j,n}$ and fixed transmit power, p_t can be written as

$$\Gamma_{j,n} = \frac{p_t |\gamma_{j,n}|^2}{\sum_{\substack{m=1 \\ m \neq n}}^N \mathbb{1}(\theta_n, \theta_m) p_t |\gamma_{j',m,n}|^2 + \sigma^2}, \quad (1)$$

$$\mathbb{1}(\theta_n, \theta_m) = \begin{cases} 1, & \text{if } \theta_n = \theta_m \\ 0, & \text{Otherwise,} \end{cases} \quad (2)$$

where $j' \in \mathcal{J}$ identifies the interfering device in subnetwork $m \in \mathcal{N}, m \neq n$ operating over the same time-frequency slot as device j in subnetwork n with the corresponding interfering channel gain, $\gamma_{j',m,n}$. σ^2 denotes the thermal noise power.

B. Conflict Graph Model of Subnetworks

The subnetwork deployment can be represented as a graph $G(\mathcal{V}, \mathcal{E})$, where the set of nodes $\mathcal{V} = \{1, 2, \dots, N\}$ represent the subnetworks and the set of edges $\mathcal{E} = \{(n, m) : n, m \in \mathcal{V}\}$ represents potential inter-subnetwork interference. An edge exists if subnetwork n and subnetwork m are considered neighbouring subnetworks, i.e. $m \in \mathbb{N}(n)$ which can be based on different rules, where $\mathbb{N}(n)$ denotes a set of the neighbours of n . Foremost, it is important that the resulting interference graph has a chromatic number of K . The chromatic number of a graph is the number of colours required to colour the nodes of the graph such that no adjacent nodes have the same colour. That is, it should be possible that all the nodes in the subnetwork conflict graph can be allocated orthogonal sub-bands such that no adjacent nodes are allocated the same sub-band given a maximum of K sub-bands. One possible approximation to consider when building the subnetwork conflict graph described in [6] is to connect each subnetwork to $K - 1$ neighbours. In this paper, we consider the following two approaches to constructing $G(\mathcal{V}, \mathcal{E})$ for the subnetwork deployment.

- Interference Graph (IG) - In this case, we consider a set \mathcal{M}_{I_n} which includes all the $K - 1$ strongest interfering subnetworks to subnetwork n . $G(\mathcal{V}, \mathcal{E})$ is built, such that;

$$\{\forall (n, m) \mid \mathcal{E}_{n,m} = 1 \text{ if } m \in \mathcal{M}_{I_n}, \text{ else } \mathcal{E}_{n,m} = 0\}, \quad (3)$$

- Signal to Interference Ratio (SIR) Graph (SG) - The SIR

of device j in subnetwork n can be defined as

$$\text{SIR}_{j,n} = \frac{p_t |\gamma_{j,n}|^2}{\sum_{\substack{m=1 \\ m \neq n}}^N \mathbb{1}(\theta_n, \theta_m) p_t |\gamma_{j',m,n}|^2}. \quad (4)$$

We consider a set \mathcal{M}_{S_n} of all the neighbours of the n th subnetwork that results in its $K - 1$ lowest SIR. In this case

$$\{\forall(n, m) \mid \mathcal{E}_{n,m} = 1 \text{ if } m \in \mathcal{M}_{S_n}, \text{ else } \mathcal{E}_{n,m} = 0\}. \quad (5)$$

C. Sub-band Allocation as a Node Classification Task

Given the subnetwork deployment conflict graph $G(\mathcal{V}, \mathcal{E})$, the node $n \in \mathcal{V}$ is labelled by the sub-band selection θ_n . The optimization problem is to select θ_n, θ_m such that $\mathbb{1}(\theta_n, \theta_m) = 0$ if $m \in \mathbb{N}(n) \forall n$ which would intuitively minimize mutual inter-subnetwork interference for the n th subnetwork if $\mathbb{N}(n) = \mathcal{M}_{I_n}$, or maximize SIR, if $\mathbb{N}(n) = \mathcal{M}_{S_n}$. This optimization problem is similar to graph colouring [8]. The graph colouring problem has been statistically analyzed using the physics anti-ferromagnetic Potts spin model [16]. According to [16], the Potts model on a graph $G(\mathcal{V}, \mathcal{E})$ defines the Hamiltonian of the interaction between adjacent nodes n, m with spin variables $\eta_n, \eta_m \in \{1, 2, \dots, K\}$ as

$$\mathcal{H}(\eta) = \sum_{(n,m) \in \mathcal{E}} \delta(\eta_n, \eta_m), \quad (6)$$

where, $\delta(\eta_n, \eta_m) = 0$ if $\eta_n \neq \eta_m$, which implies that the energy contribution of adjacent spins with different spin variables is zero, and positive otherwise. Essentially, if $G(\mathcal{V}, \mathcal{E})$ is K -colourable, to achieve a ground state energy of zero, the model penalizes adjacent spins that have the same spin variables. In relation, we can consider the sub-band allocation θ_n as a one-hot code for a spin variable η_n given the subnetwork conflict graph. According to [17], the Hamiltonian can be reformulated in terms of the one-hot vector θ_n to derive the loss function [17]

$$\min_{\Theta} L(\theta_n) = \sum_{(n,m) \in \mathcal{E}} \theta_n^T \cdot \theta_m. \quad (7)$$

This loss function would have a minimum value of zero if all the adjacent subnetworks are allocated orthogonal subbands, i.e. if $\theta_n \neq \theta_m \forall (n, m) \in \mathcal{E}$ corresponding to equation (6). For the unsupervised procedure that minimizes (7), we redefine the problem as a multi-class node classification, where a class is a sub-band. To enable a differentiable procedure, we replace the one-hot vector with a normalized smooth approximation of its class, $\theta_n \mapsto \hat{\theta}_n \in [0, 1]^K$. Hence,

$$\min_{\hat{\Theta}} L(\hat{\theta}_n) = \sum_{(n,m) \in \mathcal{E}} \hat{\theta}_n^T \cdot \hat{\theta}_m \quad (8)$$

The next section proposes the graph-driven model to learn $\hat{\theta}$ and describes the training procedure.

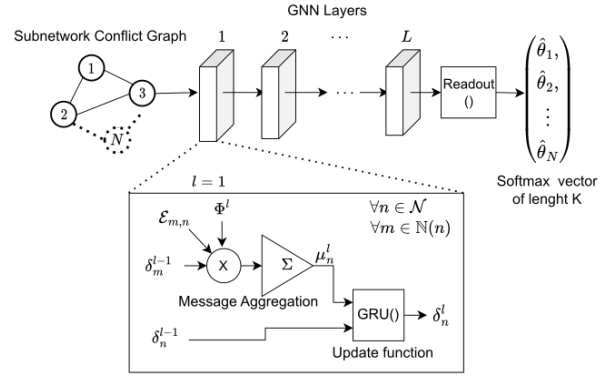


Fig. 2. Graph Neural Network Design

III. SUB-BAND ALLOCATION USING GRAPH NEURAL NETWORK

GNN is a family of neural network algorithms capable of learning from graph signals. As shown in figure 2, the GNN architecture consists of L layers. The propagation model in a GNN layer can be described using two functions, the message aggregation function and the update function. The message aggregation function is a permutation equivariant function that aggregates a pairwise exchange of embeddings between adjacent nodes. The update function generates a new embedding for the node from the aggregated messages. For the design of the message aggregation and update functions, we adopted the following Gated Graph Neural Network architecture (GGNN) [18].

A. Gated Graph Neural Network Architecture

Given the conflict graph of the subnetwork deployment $G(\mathcal{V}, \mathcal{E})$, the aggregated message for each node $n \in \mathcal{V}$ at layer $l \in \{1, 2, \dots, L\}$ as illustrated in figure 2 is given as;

$$\mu_n^l = \sum_{m \in \mathbb{N}(n)} \mathcal{E}_{m,n} \cdot \Phi^l \cdot \delta_m^{l-1}, \quad (9)$$

where Φ^l is the trainable feature transformation weight matrix of the message aggregation function, and δ_m^{l-1} denotes the previous node embedding of the neighbour. The update function is implemented using a gated recurrent unit (GRU), where the input is the aggregated message and the hidden state is the previous node embedding. So, the new embedding of node n at layer l is given as

$$\delta_n^l = \text{GRU}(\mu_n^l, \delta_n^{l-1}). \quad (10)$$

The GRU function consists of the reset gate r^l , update gate u^l and the new gates o^l which are define as

$$\begin{aligned} r^l &= \sigma(A_r^l \mu_n^l + a_r^l + B_r^l \delta_n^{l-1} + b_r^l), \\ u^l &= \sigma(A_u^l \mu_n^l + a_u^l + B_u^l \delta_n^{l-1} + b_u^l), \\ o^l &= \tau(A_o^l \mu_n^l + a_o^l + r^l \otimes (B_o^l \delta_n^{l-1} + b_o^l)), \end{aligned} \quad (11)$$

where $\sigma(\cdot)$ is a sigmoid activation function, $\tau(\cdot)$ is a hyperbolic tangent activation function. $A_r^l, B_r^l, A_u^l, B_u^l, A_o^l, B_o^l$

are trainable weights of the reset gate, update gate and new gate respectively, $a_r^l, b_r^l, a_u^l, b_u^l, a_o^l, b_o^l$ are their corresponding biases. The update function in (10) is then given as

$$\delta_n^l = (1 - u^l) \otimes o^l + u^l \otimes \delta_n^{l-1}, \quad (12)$$

where \otimes denotes Hadamard product.

The trainable message aggregation weight allows the GGNN to learn the representation of the input graph structure while the update GRU allows the GGNN to learn the relationship between different intermediate internal embeddings in the L layers [18].

Finally, a readout function compresses the final node embedding after L GGNN layers into a normalized soft vector of size K , $\hat{\theta}_n$ as in

$$\hat{\theta}_n = \text{Softmax}(W\delta_n^L + b), \quad (13)$$

where W and b are the weights and biases of the readout function.

B. Training and Execution Procedure

We employed an unsupervised training algorithm which does not depend on any ground truth. The training graphs are generated using the conflict graph model of the subnetworks. A mini-batch of graphs is propagated through the GGNN layers which execute (9), (10), and (13). The output $\hat{\theta}_n \forall n$ is passed to the loss function (8). By using mini-batch gradient descent, the $\hat{\theta}_n$ at training iteration t , $\hat{\theta}_n^t$ is updated as in

$$\hat{\theta}_n^t = \hat{\theta}_n^{t-1} - \vartheta \mathbb{E}_{\mathcal{B}} \nabla_{\hat{\theta}_n} L(\hat{\theta}_n^{t-1}) \quad (14)$$

The training is terminated when $\mathbb{E}_{\mathcal{B}}(L(\hat{\theta}_n^t) - L(\hat{\theta}_n^{t-1})) < \epsilon$, where ϵ is the error tolerance, $\mathbb{E}_{\mathcal{B}}$ is the expectation over the batch of graph, and ϑ is the learning rate.

Since the input graphs have no attributes, all nodes are treated equally, hence the prediction depends on the structure of the graph which is learned during the message-passing procedure. The predicted sub-band for subnetwork n is given as $\text{argmax}(\hat{\theta}_n)$.

The trained model can be executed in a centralized or decentralized manner. For decentralized execution, each subnetwork obtains a copy of the trained GGNN model and executes layer l to obtain embedding δ_n^l based on the message δ_m^{l-1} received from neighbouring subnetworks. Hence, such implementation would require L rounds of such message passing and the size of each message depends on the size of the embedding. This however would incur considerable signalling overhead and require synchronization between the subnetworks in executing each GGNN layer. On the other hand, centralized execution could be preferred if the subnetworks are within the coverage of a central network. In this case, the central network controller obtains the $K - 1$ neighbour identifiers for all subnetworks, builds the conflict graph, executes the trained GGNN model, and signals the sub-band selection decision to the subnetworks.

IV. RESULTS AND DISCUSSION

In this section, we discuss the simulation assumption for the subnetwork deployment, the GGNN model selection and train-

TABLE I
SIMULATION ASSUMPTION

Parameter	Value	Parameter	Value
Factory area	40m x 25m	Number of subnetworks	50
Subnetwork radius	2.5m	Number of devices per subnetwork	1
Minimum distance between APs	2.5m	Device to AP minimum distance	1m
InF-DL clutter density, clutter size	0.6, 2	Correlation distance	10m
Shadowing std (LOS, NLOS)	4dB, 7.2dB	Path loss exponent (LOS, NLOS)	2.15, 3.57
Transmit power	0 dBm	Number of subbands	5
Total bandwidth	20 MHz	Center frequency	28 GHz
Noise figure	10 dB	Number of GGNN layers	10
Size of embedding	64	Training epochs	500
Training data size	50000	Batch size	64
Initial learning rate	10^{-3}	Optimizer	ADAM

ing parameters shown in table I, including brief descriptions of the benchmark algorithms. We compare the performance of the various benchmarks and our proposed approach in terms of the network spectral efficiency, execution complexity and generalizability. For the graph-based methods, we consider the two subnetwork conflict graphs construction methods IG and SG discussed in section 2.B. The spectral efficiency (SE) (bits/s/Hz) is approximated using Shannon capacity as $\text{SE}_{j,n} = \log_2(1 + \Gamma_{j,n})$.

A. Simulation Assumptions

1) *Subnetwork Deployment*: To evaluate the proposed method, we randomly deploy $N = 50$ subnetworks in a factory floor of size $40m \times 25m$ resulting in a density of 50000 subnetworks/km². We consider $K = 5$ sub-bands. To model the large-scale fading, we used the 3GPP TR 38.901 Indoor Factory (InF) channel model [19] for the Dense-clutter Low-antenna (InF-DL) scenario and the associated model for the probability of non-line of sight (NLOS) and line of sight (LOS). The InF-DL scenario is appropriate since the subnetwork's AP and the devices are clutter-embedded. We consider full buffer uplink transmission. The transmission link path-loss ρ is represented by the alpha-beta-gamma model [19]. The shadow fading s is modelled using the spatially correlated shadowing model used in [14]. The small-scale fading is Rayleigh distributed and complex-valued, denoted as $h \sim \mathcal{CN}(0, 1)$. Finally, the corresponding channel gain is then calculated as $\gamma = h \times \sqrt{10^{(\rho+s)/10}}$.

2) *GGNN Model and Training Settings*: The GGNN model is implemented with PyTorch Geometric and comprises $L = 10$ layers, with each layer having an output node embedding of size 64. The model is trained with a batch of 64 graphs and a total of 50000 graphs for 500 epochs, using the Adaptive Moment Estimation (ADAM) optimizer with an initial learning rate of 10^{-3} . The parameters for training and model selection as shown in table I were chosen based on experimental validation.

B. Benchmarks

To evaluate the performance of our proposed scheme in improving the network performance, we compare it with the following schemes;

- 1) Random Allocation (RA) - A distributed scheme where one sub-band is randomly selected from the available K options for each subnetwork.

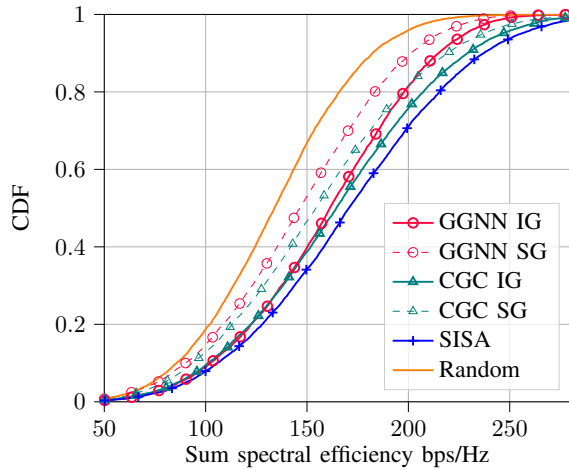


Fig. 3. Cumulative distribution function (CDF) of the sum spectral efficiency for 10000 test snapshots

- 2) Sequential Iterative Sub-band Allocation (SISA) - The sub-band selection sequential algorithm for subnetworks as detailed in [11] is a centralized iterative algorithm that minimizes the sum of the weighted interference.
- 3) Centralized Graph Coloring (CGC) - The approach described in [12] applies a greedy graph colouring heuristic for sub-band allocation in subnetworks. We applied this method to the same conflict graph used for evaluating our proposed graph-based learning technique.

C. Network Performance Evaluation

Figures 3 and 4 show the empirical cumulative distribution function (CDF) of the sum SE and per-device SE, respectively, for the proposed scheme and the different benchmarks tested with 10000 network realizations. Given IG, our proposed method outperforms random sub-band allocation by 20% in terms of achievable sum SE at the median. Below the median, GGNN achieves the same performance as CGC and lags behind SISA by 8%. However, note that SISA requires full channel gain information of all the mutual interfering links and desired links. Furthermore, we can achieve a notable gain in per-device SE by up to 33% at the median, and multiply the 1% per-device SE by a factor of 3 ($3\times$) compared to random sub-band allocation as shown in figure 4. The *SG* graph construction can improve performance in the lower percentiles of per-device SE at the expense of the upper percentiles. For example, we can enhance the 1% per-device SE by up to $5\times$ using GGNN. This performance is comparable to CGC, and only marginally lower than SISA which can achieve a $6\times$ increase in 1% per-device SE compared to random sub-band allocation.

D. Complexity Analysis

We analyzed the complexity of our proposed GGNN method and compared it with the benchmark algorithms, CGC and SISA in terms of the computational runtime and signalling

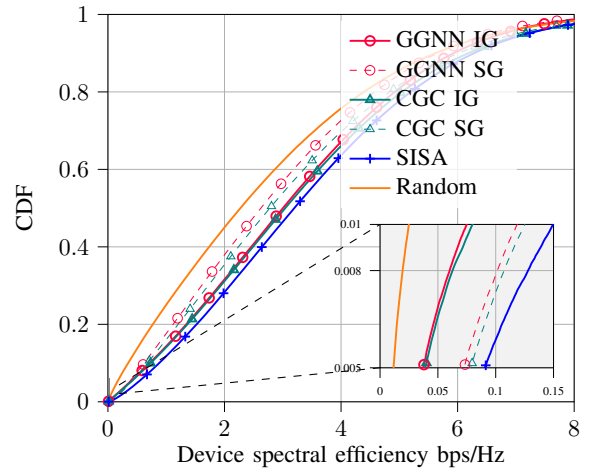


Fig. 4. Cumulative distribution function (CDF) of the per-device spectral efficiency for 10000 test snapshots

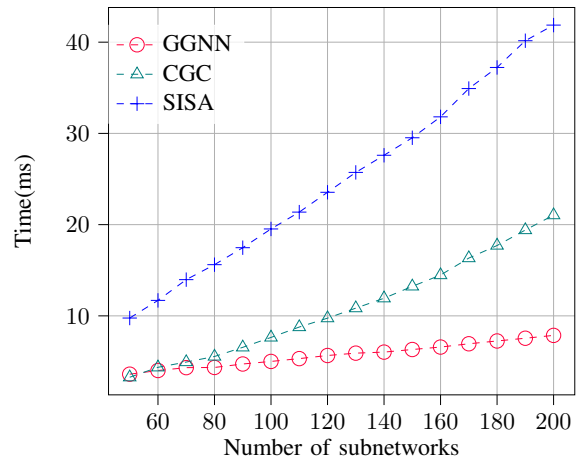


Fig. 5. Computational runtime for different number of subnetworks (ms) averaged over 10000 realizations

requirement. Each algorithm is developed with Python frameworks and ran on a Windows machine with an 11th Gen Intel(R) Core(TM) i7-11850H @ 2.50GHz processor and 32G memory. The result of the runtime analysis for different numbers of subnetworks, $N \in \{50, 60, \dots, 200\}$ in figure 5 is averaged over 10000 realizations. As shown in the figure, our GGNN method has a faster runtime, growing at a slower linear rate compared to the SISA and CGC. Hence, it would be more suitable for very dense networks with a large number of subnetworks or APs. While the runtime analysis is carried out on a CPU, it is expected that the runtime for the GGNN method would further decrease on a GPU.

For the signalling overhead considering centralized implementation, the GGNN requires less information and therefore incurs fewer signalling resources than SISA. For example, N^2 signalling messages are required to be signalled to the central resource management entity from N subnetworks to execute the SISA algorithm; on the other hand, the GGNN method

TABLE II

GENERALIZABILITY OF THE PROPOSED METHOD TO DIFFERENT NETWORK SETTINGS AND CHANNEL MODEL IN TERMS OF AVERAGE RATE (BPS/HZ)

		Test		
		Default	Scenario 1	Scenario 2
Train	Default	2.9445	2.8167	6.1154
	Scenario 1	2.9403	2.8124	6.1100
	Scenario 2	2.9298	2.7965	6.1238

only requires $N(K-1)$ signalling messages, where $K \ll N$ in a large network. This further justifies the suitability of the proposed method for a large-scale deployment of subnetworks.

E. Generalizability

We analyze the ability of the proposed graph-based learning method to generalize to different network settings and channel models different from the training system model assumption as shown in table II. The default scenario is as presented in table I and we consider two different scenarios. Scenario 1 is a network consisting of 80 subnetworks deployed in a $50m \times 30m$ area, resulting in a 53300 subnetworks/ km^2 density, with the channel model based on 3GPP in-factory sparse clutter low antenna (InF-SL) model [19]. The NLOS path loss exponent, shadow fading standard deviation, clutter size and clutter density are 2.55, 5.7 dB, 10 and 0.35 respectively. Scenario 2 involves a less dense deployment of 20 subnetworks in $25m \times 25m$ area, i.e. 32000 subnetworks/ km^2 with path-loss modelled following the 3GPP model for inH-Office [19]. The NLOS path loss exponent, shadow fading standard deviation, and correlation distance are 3.83, 8.03 dB, and $6m$. We train different GGNN models from training graphs constructed based on IG for a given scenario and tested on all three scenarios. As shown in table II, we observe that the average SE from testing with 10000 snapshots remain relatively the same for a test scenario, regardless of the training scenario. This shows that the trained model can generalize to different numbers of subnetworks, density and channel models. The robustness to different settings is due to the fact that the GGNN model learns based on the graph structure, which depends on the graph construction rule and not the distribution of the channel model.

V. CONCLUSION AND FUTURE WORK

This paper investigates an unsupervised graph-based learning approach to sub-band allocation for dense wireless subnetworks. The topology of the subnetwork is represented as a graph and the sub-band allocation is formulated as a node classification task parameterized by GGNN using a loss function inspired by Potts model. We propose two different conflict graph representations and show that the tradeoff of improving outage and global performance depends on the conflict graph construction rule. We show that our approach offers comparable performance and requires lower runtime and signalling overhead than the centralized benchmark heuristics. We further show that the trained GGNN model is scalable,

agnostic to the channel model and can be executed in a centralized or decentralized manner. Hence, the approach can be suitable for large-scale deployment of subnetworks. To better take advantage of the data-driven technique, our future work will consider more complex scenarios including traffic and mobility, where graph-based learning methods could outperform heuristics using the predictive ability of data-driven techniques.

REFERENCES

- [1] Z. Zhang, Y. Xiao, Z. Ma, M. Xiao, Z. Ding, X. Lei, G. K. Karagiannidis, and P. Fan, "6G Wireless Networks: Vision, Requirements, Architecture, and Key Technologies," *IEEE Vehicular Technology Magazine*, vol. 14, no. 3, pp. 28–41, 2019.
- [2] H. Viswanathan and P. E. Mogensen, "Communications in the 6G Era," *IEEE Access*, vol. 8, pp. 57 063–57 074, 2020.
- [3] R. Y. Chang, Z. Tao, J. Zhang, and C.-C. Kuo, "A Graph Approach to Dynamic Fractional Frequency Reuse (FFR) in Multi-Cell OFDMA Networks," in *2009 IEEE International Conference on Communications*, 2009, pp. 1–6.
- [4] S. Uygungelen, G. Auer, and Z. Bharucha, "Graph-based dynamic frequency reuse in femtocell networks," in *2011 IEEE 73rd Vehicular Technology Conference (VTC Spring)*, 2011, pp. 1–6.
- [5] C. Zhao, X. Xu, Z. Gao, and L. Huang, "A coloring-based cluster resource allocation for ultra dense network," in *2016 IEEE International Conference on Signal Processing, Communications and Computing (ICSPCC)*, 2016, pp. 1–5.
- [6] R. Adeogun, G. Berardinelli, I. Rodriguez, and P. Mogensen, "Distributed Dynamic Channel Allocation in 6G in-X Subnetworks for Industrial Automation," in *2020 IEEE Globecom Workshops (GC Wkshps)*, 2020, pp. 1–6.
- [7] D. Bréaz, "New methods to color the vertices of a graph," *Commun. ACM*, vol. 22, pp. 251–256, 1979.
- [8] A. Kosowski and K. Manuszewski, "Classical coloring of graphs," 2008.
- [9] O. Iacobaiea, J. Krolkowski, Z. Ben Houidi, and D. Rossi, "Real-Time Channel Management in WLANs: Deep Reinforcement Learning versus Heuristics," in *2021 IFIP Networking Conference (IFIP Networking)*, 2021, pp. 1–9.
- [10] E. Rozner, Y. Mehta, A. Akella, and L. Qiu, "Traffic-Aware Channel Assignment in Enterprise Wireless LANs," in *2007 IEEE International Conference on Network Protocols*, 2007, pp. 133–143.
- [11] D. Li, S. R. Khosravirad, T. Tao, and P. Baracca, "Advanced Frequency Resource Allocation for Industrial Wireless Control in 6G subnetworks," in *2023 IEEE Wireless Communications and Networking Conference (WCNC)*, 2023, pp. 1–6.
- [12] R. Adeogun, G. Berardinelli, and P. Mogensen, "Learning to Dynamically Allocate Radio Resources in Mobile 6G in-X Subnetworks," in *2021 IEEE 32nd Annual International Symposium on Personal, Indoor and Mobile Radio Communications (PIMRC)*, 2021, pp. 959–965.
- [13] Z. Zhang, D. Zhai, R. Zhang, and Y. Wang, "Deep neural network-based channel allocation for interference-limited wireless networks," in *2019 IEEE 20th International Conference on High-Performance Switching and Routing (HPSR)*, 2019, pp. 1–5.
- [14] R. Adeogun and G. Berardinelli, "Distributed Channel Allocation for Mobile 6G Subnetworks via Multi-Agent Deep Q-Learning," in *2023 IEEE Wireless Communications and Networking Conference (WCNC)*, 2023, pp. 1–6.
- [15] K. Nakashima, S. Kamiya, K. Ohtsu, K. Yamamoto, T. Nishio, and M. Morikura, "Deep Reinforcement Learning-Based Channel Allocation for Wireless LANs With Graph Convolutional Networks," *IEEE Access*, vol. 8, pp. 31 823–31 834, 2020.
- [16] L. Zdeborová and F. Krzakala, "Phase transitions in the coloring of random graphs," *Phys. Rev. E*, vol. 76, p. 031131, Sep 2007.
- [17] M. J. A. Schuetz, J. K. Brubaker, Z. Zhu, and H. G. Katzgraber, "Graph coloring with physics-inspired graph neural networks," *Phys. Rev. Res.*, vol. 4, p. 043131, Nov 2022.
- [18] Y. Li, R. Zemel, M. Brockschmidt, and D. Tarlow, "Gated graph sequence neural networks," in *Proceedings of ICLR'16*, April 2016.
- [19] 3GPP, "Study on channel model for frequencies from 0.5 to 100 GHz," 3rd Generation Partnership Project (3GPP), Technical Report (TR) 38.901, 04 2022, version 17.0.0.